

Supplementary Materials for

VITALS: An Implantable Sensor Network for Postoperative Cardiac Monitoring in Heart Failure Patients

Ali Kight, Moussa Haidar, Masafumi Shibata, Yoshikazu Ono,
Gentaro Ikeda, Amit Sharir, Federica Semproni, Yellappa Palagani,
Sawson Taheri, Amy Kyungwon Han, Michael Ma, Kirk Reimer,
Doff McElhinney, Seraina Dual, Mark Cutkosky

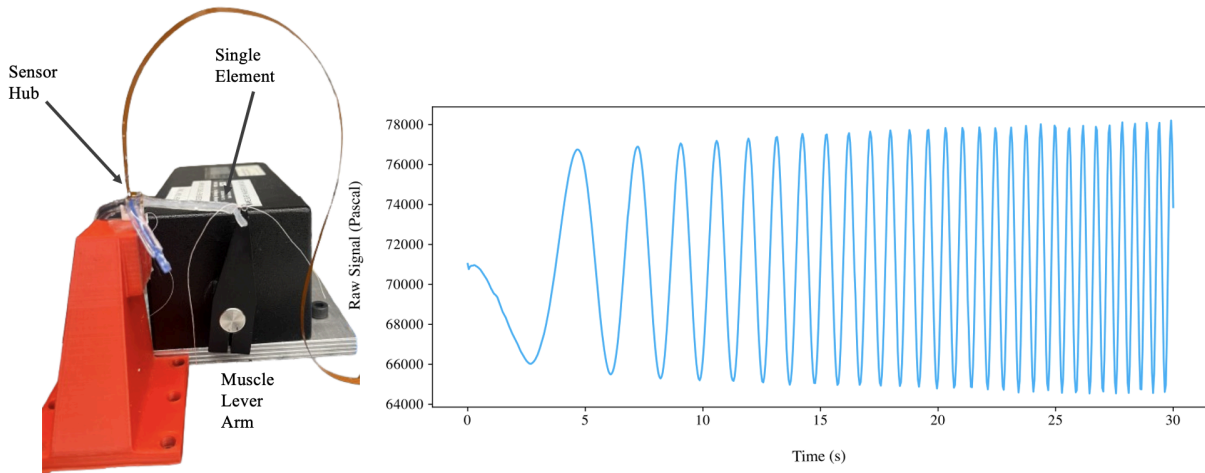


Figure S1: Sensor calibration. Each sensing element for each sensing hub was individually calibrated using an 300C Aurora Scientific Muscle lever. The sensing hub was mechanically anchored using a custom 3D-printed jig (in red). The distal end of the sensing arm is secured to the muscle lever arm using thread, keeping the arm in slight tension. The muscle-lever is prescribed a displacement signal of a 1.5 Hz sine wave of an amplitude of 5mm. This procedure yields an affine relationship between sensor signal and strain. Silicone is a viscoelastic material that exhibits slight hysteresis and dynamic stiffness. The graph displays a single sensing element cycled at 20% strain over a frequency sweep of 0-3 Hz. There is a slight increase in signal amplitude as frequency increases; however, the magnitude of signal change is equal to 0.49mm, which is less than the RMSE between sensor strain and optically tracked strain, as shown in the main text, Figure 2B. Therefore, a linear calibration is sufficient. Interested readers can refer to previous work that developed a transfer function that compensated for hysteresis (34). The calibration for each element is integrated into the microcontroller firmware, and the strain output for each axis is the average of the two opposing sensing elements.

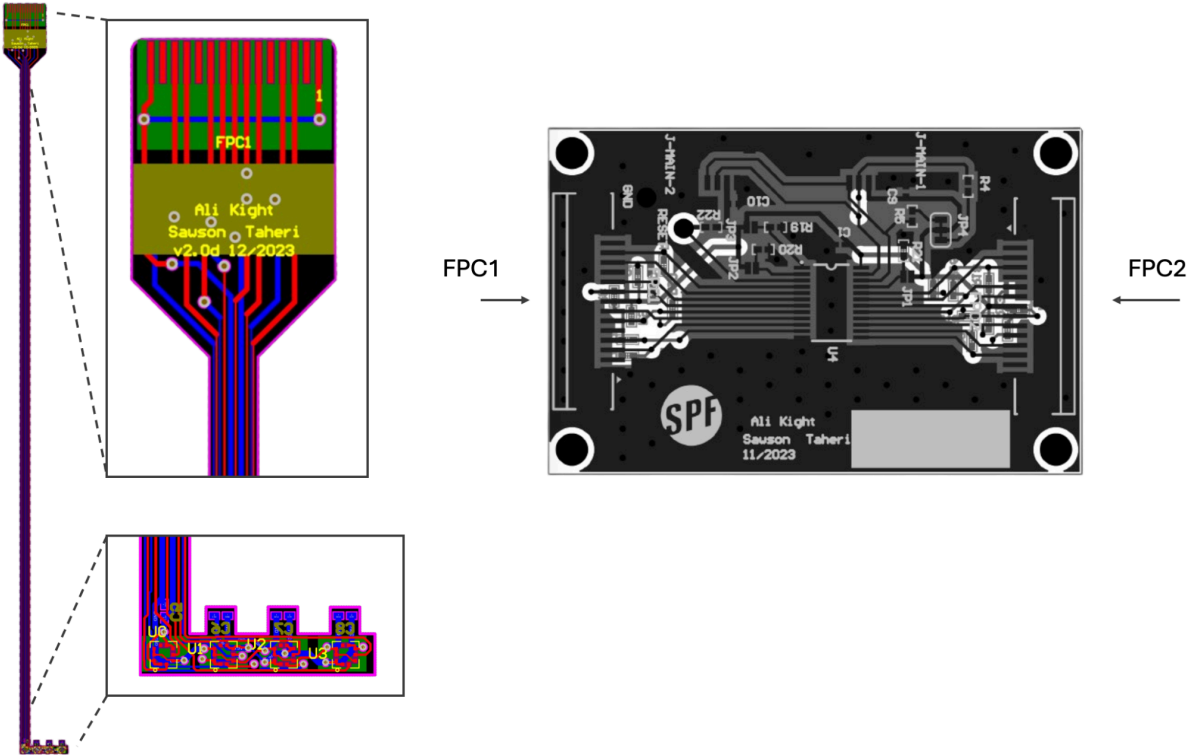


Figure S2: PCB layout for the LV and RV sensing hubs. Each of the LV and RV sensing hubs consists of a single flex printed circuit (flex PCB) that hosts four MEMS barometers. Communication with these barometers is facilitated through the I2C protocol, with each MEMS barometer being sequentially addressed through a multiplexer. This arrangement is necessary because the specific barometers used (Bosch BMP384) support only two distinct addresses, requiring use of a multiplexer for selective communication. A custom board was designed and manufactured, incorporating flexible printed circuit connectors for each hub. These connectors are designed to ensure robust electrical connections, while the elongated and slender flex PCB wiring leading to the barometers provides necessary strain and torque relief, enhancing the system's durability and reliability in dynamic environments.

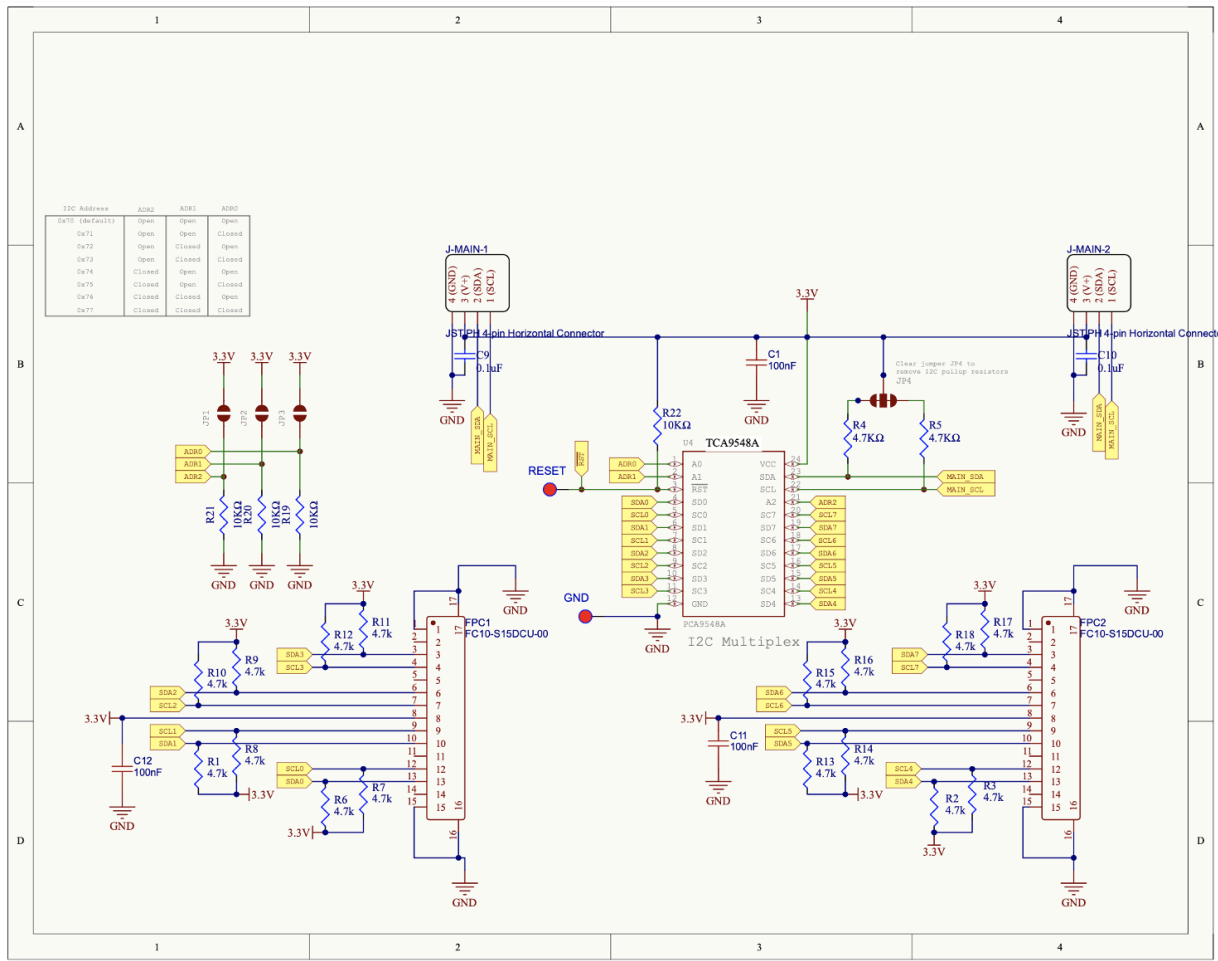


Figure S3: Circuit schematic for FPC connectors and multiplexer. The diagram illustrates the circuit components and connectivity between the LV and RV sensing hub FPC fingers and the 8-channel multiplexer. Additional 4-pin connectors are integrated into the FPC multiplexer board, facilitating the series connection with the multiplexer dedicated to the aortic sensor.

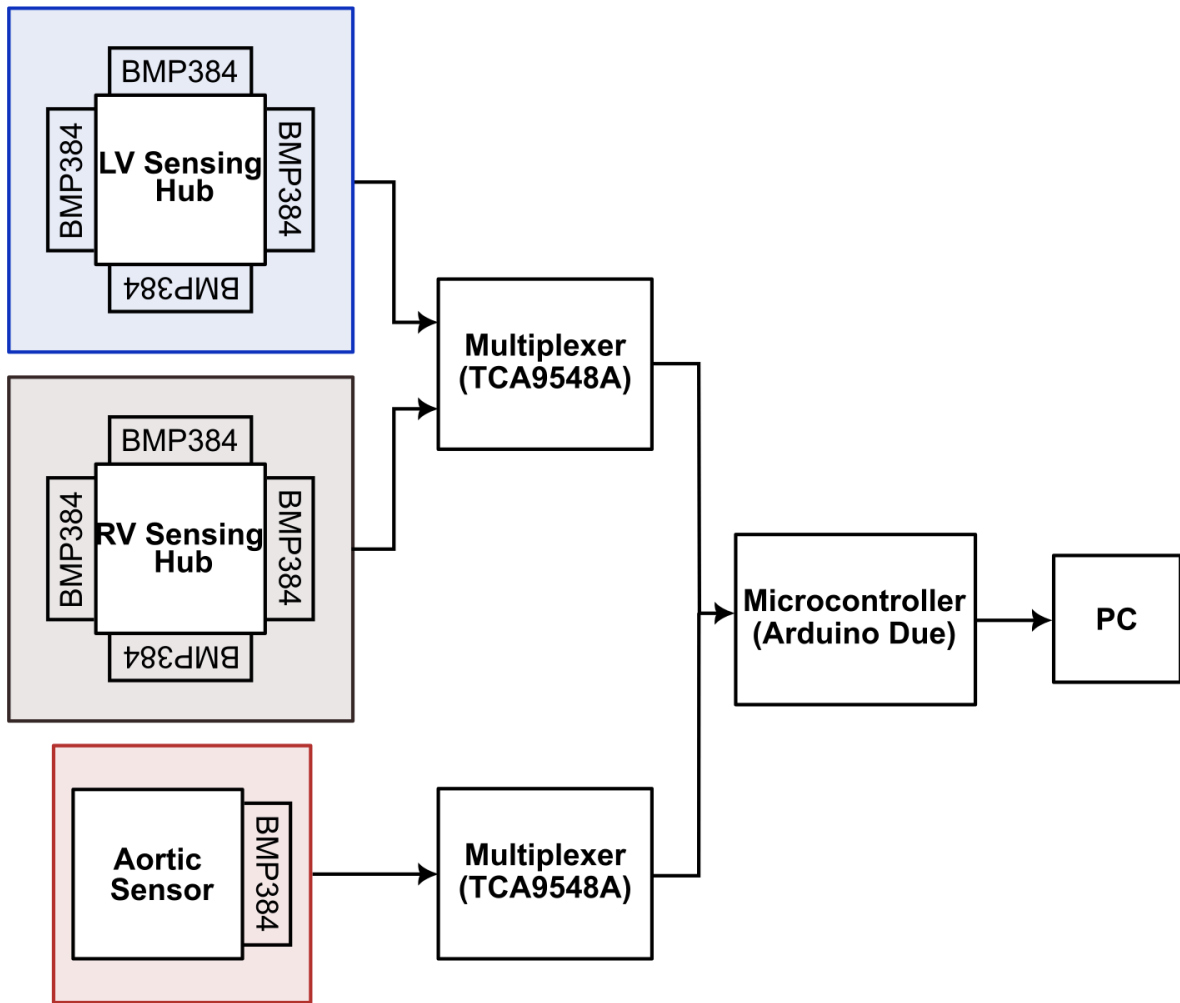
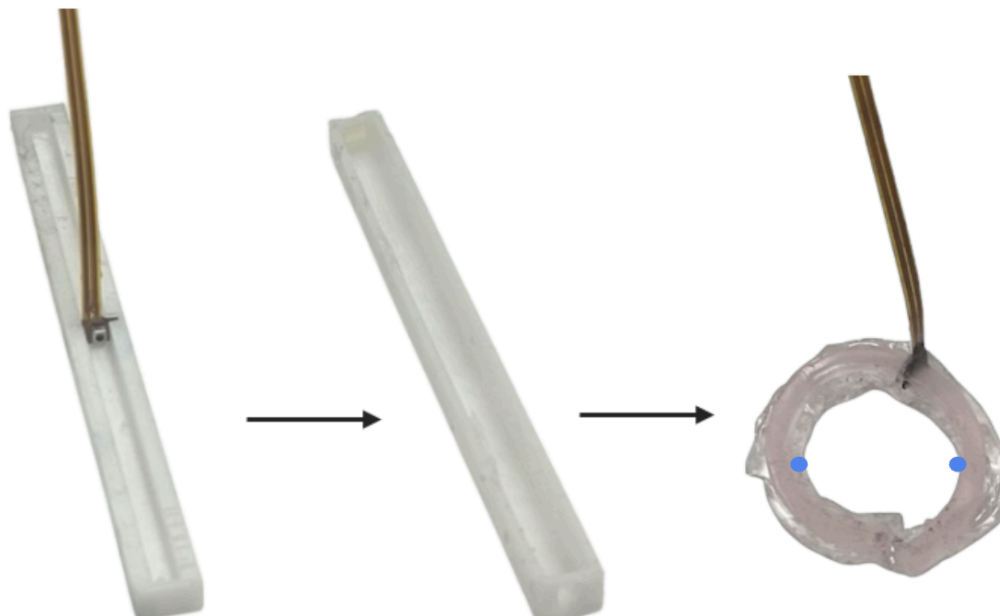


Figure S4: VITALS network system diagram. The system is designed for efficient communication and data processing from multiple sensors. The LV and RV sensing hubs communicate through an 8-channel I₂C multiplexer. Additionally, there is a separate multiplexer dedicated to the aortic sensor. The dual multiplexer setup enables both hubs and the aortic sensor to share a singular clock and data line leading to the microcontroller, optimizing efficiency but enabling stable, secure readout. The data is read from the microcontroller and transmitted in real-time to a custom MATLAB interface at a rate of 66 Hz.



Cast Silicone Cast Gel Encircle Vessel

Figure S5: Fabrication of aortic sensor for VITALS network. The aortic sensor is fabricated in a similar fashion to the LV and RV hubs but it contains only a single MEMS barometer. The sensing element is case with silicone, and post-cure, the structure is encapsulated with the silicone gel. Only one side of the aortic sensor is instrumented with a barometer. The additional element provides counter-tension for PCB stabilization and complete encirclement of the vessel. The sensor is sutured in two locations to the aortic adventitia, denoted by the blue dots. The rough edges of the sensor can be attributed to flash during the casting process, leaving extra material on the sensor's outer gel coating. The effect of this extra material is compensated for during calibration *in situ*.

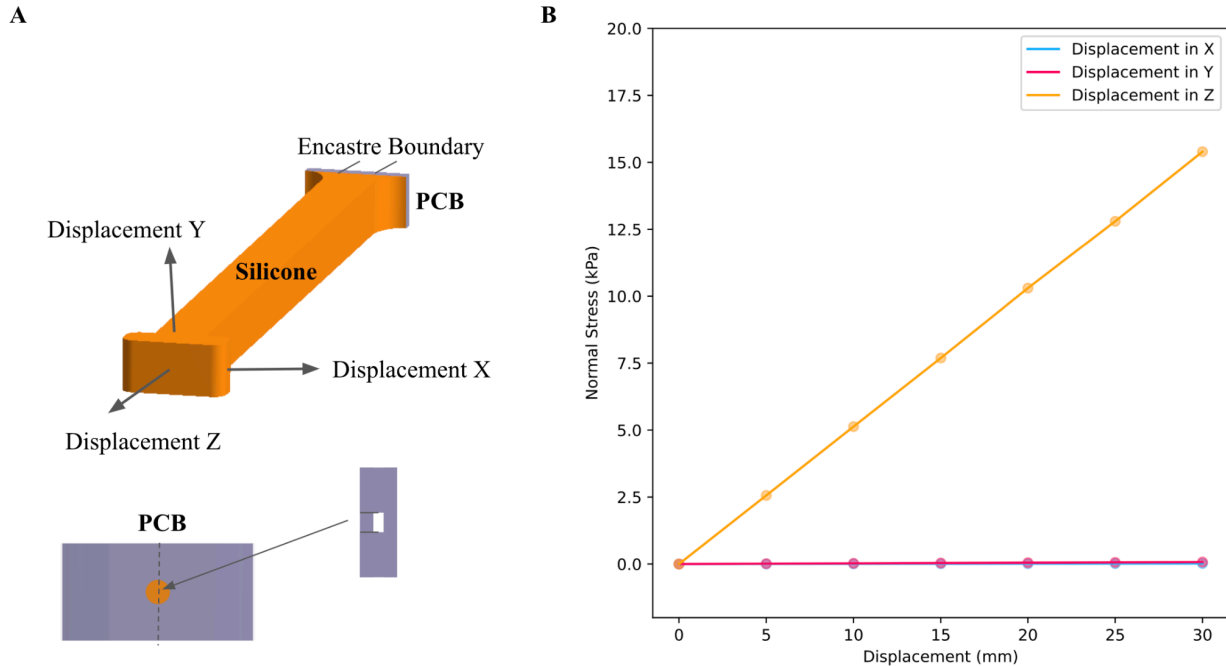


Figure S6: Finite element modeling of a sensing element. (A) Illustration of the finite element model setup using a mesh-less mechanical analysis software, SimSolid (101). The structure includes a silicone element modeled as a linear elastic solid, with Young's modulus determined by the manufacturer's specifications for Ecoflex 00-10 silicone (55 kPa), and a PCB modeled with an effectively inextensible material (1 GPa). The PCB represents the MEMS barometer, with a circular plate delineated in the middle of the PCB and an air cavity behind it, a simplified representation of the MEMS capacitor. The end of the silicone is displaced, and normal stress on the circular segment is measured to represent the signal. **(B)** Graph of normal stress as a function of sensor displacement. The Z-axis represents the axial direction of strain, where displacement linearly contributes to the signal, aligning with experimental results (34). Displacement in orthogonal directions, which would result in bending of the structure, results in negligible stresses on the PCB-silicone interface. This is due to the sensor's low bending stiffness, contributing little to the stress on the PCB.

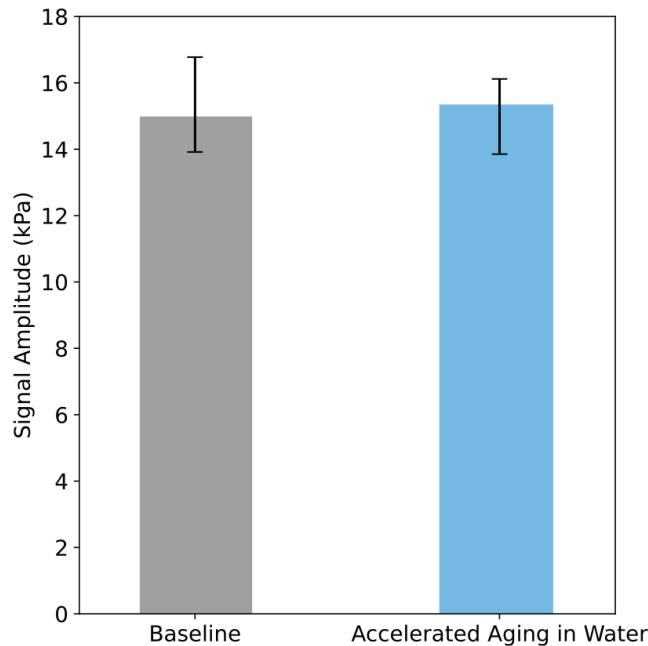


Figure S7: Accelerated age testing of silicone-coated VITALS circuitry. We tested a single MEMS barometer and associated circuitry cast with a 40 mm long silicone element submerged in physiological saline. The testing was conducted at 80 degrees Celsius over 78 hours, which is proportional to approximately 68 days at body temperature (3). The sensor was cycled at 25% strain before and after accelerated aging, and signal amplitude was calculated. No statistically significant change in signal was observed, with a two-tailed P value of 0.6698.

Movie S1: Implantation and data collection on large animal model. This video demonstrates the implantation of the right ventricular sensing hub onto the epicardium, followed by the full implantation of both ventricular sensing hubs. It then visualizes the real-time signals generated by VITALS, including two-axis readings from each ventricle and an aortic pressure reading.